Local order and dynamics in supercooled water: A study by IR spectroscopy and molecular dynamic simulations

Alexander Yu. Zasetsky, Alexei F. Khalizov, and James J. Sloan

Citation: The Journal of Chemical Physics **121**, 6941 (2004); doi: 10.1063/1.1787494
View online: http://dx.doi.org/10.1063/1.1787494
View Table of Contents: http://scitation.aip.org/content/aip/journal/jcp/121/14?ver=pdfcov
Published by the AIP Publishing

Local order and dynamics in supercooled water: A study by IR spectroscopy and molecular dynamic simulations

Alexander Yu. Zasetsky, Alexei F. Khalizov, and James J. Sloan
Department of Chemistry, University of Waterloo, Waterloo ONT N2L 3G1, Canada

(Received 6 May 2004; accepted 7 July 2004)

Micron-sized water droplets in a cryogenic flow tube were probed by IR spectroscopy. The analysis of the IR spectra suggests that there is a relative increase of about 30% in the fraction, f_L, of low density domains in water on cooling over the temperature range between 300 and 240 K. The results derived from the experiments agree qualitatively with those of molecular dynamics (MD) simulations in terms of the increase in the f_L values. The MD simulations show that the intensities of the mode at about 100 cm^{-1} for the molecules in the low density domains are reduced in comparison to the average, while the intensities and frequencies of the librational mode at 600 cm^{-1} are increased. Furthermore, the reorientations (dielectric relaxation times) in these domains are found to be somewhat slower, pointing to the fact that these low density ''cages'' live longer than the average local molecular environments in supercooled water. © *2004 American Institute of Physics.* [DOI: 10.1063/1.1787494]

I. INTRODUCTION

The vast majority of upper atmosphere aerosols and clouds are composed of water and aqueous solutions. These small particles exist in a wide variety of forms ranging from submicron condensation nuclei to submillimeter cloud droplets. These particles are believed to affect the global climate in many ways. Notable examples include the effects on the Earth's radiative budget[1] via absorption and reflection of the solar radiation and polar ozone depletion by the formation of active species through heterogeneous reactions on the aerosol surfaces.[2,3] Owing to their small volume, a considerable fraction of these aqueous aerosols may remain for long periods of time in the metastable state (supercooled liquid) under the thermodynamic conditions of the upper troposphere and lower stratosphere. The focus of the present work is on small supercooled liquid water particles at ambient pressure.

Although great progress in understanding of the thermodynamics and kinetics of water on cooling has been made in the last several decades, the origin of the unusual physical and chemical properties of water at lower temperatures is not well understood.[4–6] Yet, the mechanisms of the freezing transition in water aerosols is the subject of current discussion.[7] There are significant differences in the experimental values of the homogeneous nucleation rates for water[8–11] and ice[12–15] and those predicted by the classical nucleation theory.

During recent investigations of the size dependence of homogeneous nucleation rates using IR spectroscopic measurements on water aerosols in a cryogenic flow tube, our analysis procedure identified a very substantial fraction of ice under conditions where only supercooled liquid water would be expected. This may suggest that supercooled water contains a spectroscopically identifiable component in addition to ''normal'' water.

This would have important practical aspects, as the experimental indices of refraction are routinely used in processing remote sensing measurements of condensed phases in the atmosphere. Spectral data for supercooled water in the mid-IR, however, are not available for temperatures between 239 and 273 K. This deficiency, which is due to the difficulty in measuring the spectrum of supercooled water and deriving its optical constants, may result in incorrect retrievals of the phase and density of cirrus and deep convective clouds. The spectral picture of water aerosols in the upper atmosphere is habitually associated with a mixed phase,[16] which is the sum of the spectral contributions of hexagonal ice and normal liquid water. This approach uses the refractive indices of ice, either spliced together from parts measured at different temperatures[17] or measured at very low temperature,[18] and of liquid water measured at room temperature.[19] Although this approach seems to be adequate in many cases, it may lead to substantial uncertainty in the treatment of the spectra of supercooled water samples.

Motivated by our experimental results, we have carried out a number of molecular dynamics (MD) studies that provided insight into the origin of the changes in spectral densities in the microwave and IR regions caused by water expansion on cooling. The phenomenon of freezing nucleation is not normally observed in computer simulations owing to short simulation times and small sample sizes, although some characteristics of the local order and dynamics in water on deep supercooling can be revealed.[20–23] In fact, low density domains were observed in previous computer simulations of supercooled water[20] and an increase in the ''low density liquid'' fraction with decreasing temperature was also observed in neutron scattering experiments.[24] These results appear to imply that the variations observed in our IR absorption spectra are a manifestation of collective processes involving slow density fluctuations leading to changes in the local order in supercooled water.

The central objective of the present paper is to examine these low density domains (local molecular configurations)

and their connection to molecular dynamics in supercooled water. The remainder of this paper is organized as follows: The following Sec. II describes the experimental apparatus and the procedure for calculations of the particles size distribution and composition. Section III describes the details of the MD simulations. The results are discussed in Sec. IV, where the fraction of low density domains is estimated. We also consider the changes in the dielectric relaxation and librational motion of H_2O molecules caused by the formation of these local low density domains in water on supercooling. Section V presents the conclusions.

II. EXPERIMENT AND CALCULATIONS

A. Experimental apparatus

Experimental IR spectra of liquid supercooled water and ice aerosols were recorded using a cryogenic flow tube, which is a redesigned and improved version of the apparatus that was described previously.[25] The flow tube has four independently coolable sections, each of which is a copper pipe 38 cm long, with an inner diameter of 9 cm. The adjacent sections are separated by thin-walled stainless steel bellows that enable the generation and maintenance of a wide variety of axial temperature profiles. Each section is independently cooled by a flow of chilled gaseous nitrogen at a pressure of 7 bar. The nitrogen flow passes through two concentric coils of 6 mm copper tubing fixed to the outside of each section with thermally conductive epoxy (T7109, Epoxy Technology, Inc.). The entire assembly is enclosed in an evacuated jacket to provide thermal isolation. Electrical heaters located at the inlet cooling lines of each section are used for fine temperature control. The temperature profile is monitored using 16 T-type thermocouples—four per section—attached to the wall of the copper tube. The thermocouples and heaters are integrated via a field point modular distributed I/O interface (National instruments FP-1601, FB-TC-120, and FP-TE-10) and operated by LABVIEW code, allowing accurate thermal control. The temperature deviations along a section are within ± 0.5 K. For moderate temperature differences between sections, the aerosol particles flowing in a section attain the wall temperature of that section (within ± 0.5 K) after not more than one quarter of the section length.

Water particles generated externally were introduced in a nitrogen flow (0.5–3.0 SLPM) through a heated inlet at the top of the flow tube where they were mixed with additional nitrogen carrier gas (3–15 SLPM) to adjust the relative humidity. Smaller particles (0.3–1.5 μm) were produced by a constant output atomizer (TSI 3076, TSI Inc.), while an ultrasonic nebulizer (UltaNeb 99, De Vilbiss Co.) was used to generate particles in the range between 0.5 and 8 μm. After conditioning in the first section at 283 K, the particles were cooled in the subsequent sections to the desired temperatures (230–278 K). IR spectra were recorded through the optical ports in the bottom section using a single-pass optical configuration. A collimated IR beam modulated by a Michelson interferometer (Bruker Tensor 37) entered the observation cell through a KRS-5 window and passed across the flow before exiting through another window into a detector box, where it was focused by an off-axis parabolic mirror onto an MCT detector (FTIR-22-1.0, Infrared Associates). The spectral data then were processed using Bruker OPUS software. Each spectrum is an average of 80 scans collected in the frequency range from 450 to 6000 cm^{-1}, at 2 cm^{-1} resolution and 40 kHz metrology frequency. To obtain the pure aerosol spectra, water vapor spectra recorded at the same temperatures were subtracted from the measured extinction spectra.

B. Particle size distribution

This section describes the procedure for determination of the droplet size from IR extinction spectra. It rests upon the relationship between light scattering by small droplets suspended in gas and their sizes. In the present case of liquid particles we use the spherical approximation (Mie theory[26]) to calculate the extinction spectra for particles of different sizes. Assuming single scattering, which is appropriate for the aerosol number densities considered here (on the order of 10^6 cm^{-3}), the following least squares minimization problem with constraints can be formulated:[27]

$$\underset{\mathbf{p}}{\text{minimize}}\{|\mathbf{K}\cdot\mathbf{P}-\boldsymbol{\tau}+\gamma\cdot\mathbf{S}\cdot\mathbf{P}|^2\}^{1/2}, \quad \text{subject to } \mathbf{1}\cdot\mathbf{P}\geqslant\mathbf{0}, \quad (1)$$

where $K_{i,j}=\pi r_i^2 Q[r_i, n^*(\nu_j)]$ is the aerosol extinction cross section, $Q[\cdots]$ is the extinction efficiency, $n^*(\nu)$ is the refractive index, r is the particle radius, ν is the frequency, and $\tau(\nu)$ is the extinction spectrum. The solution vector $\mathbf{P}$ gives the particle size distribution after appropriate normalization by the volume, area, or particle number density.

The term $\gamma\cdot\mathbf{S}\cdot\mathbf{P}$ is added to deal with a rank deficiency of the matrix $\mathbf{K}$. This degeneracy results from the similarity of the spectra for relatively small particles that have small scattering intensities and identical absorption intensities. The matrix $\mathbf{S}$,

$$\mathbf{S}=\begin{vmatrix} 1 & -3 & 3 & -1 & & & & \\ & 1 & -3 & 3 & -1 & & & \\ & & . & . & . & . & & \\ & & & & 1 & -3 & 3 & -1 \end{vmatrix}, \quad (2)$$

is designed to minimize the third derivatives of $\mathbf{P}$ thus introducing a ''smoothness constraint'' on the solution vector $\mathbf{P}$. The parameter γ controls the degree of smoothness and, as a rule, is very small. The non-negativity constraint $\mathbf{1}\cdot\mathbf{P}\geqslant\mathbf{0}$, where $\mathbf{1}$ is the identity matrix, assures that all spectral intensities are positive or zero.

The set of reference spectra (column vectors of the matrix $\mathbf{K}$) is computed using the Bohren and Huffman code[26] with refractive indices $n^*(\nu)$ taken from laboratory measurements for liquid water[19] and ice.[17,18] In this study, $\mathbf{K}$ is an $N\times M$ matrix, where N is the number of frequencies ($\sim$5000) and M is the number of discrete radii. For this work, we use the spectra set for 96 radii, covering the particle size range from 0.05 to 11.88 μm.

The non-negative least squares problem is solved iteratively. The computational details and proof of convergence for the procedure can be found in Ref. 28. The uncertainty in

determination of particle radii is calculated by the standard procedure used for the least squares fitting. The error values are in the range from 0.1 (for radii between 0.5 and 4 μm) to 0.3 μm (for the particles having radius less than 0.5 or greater than 4 μm). We note that the procedure allows us to determine simultaneously the chemical composition, phase (solid or liquid), and size distribution of an aerosol sample, based on its IR extinction spectrum. The chemical components of the aerosol particles may include any material for which the wavelength-dependent indices of refraction have been determined. For the present purposes, we focus only on water.

III. COMPUTATION METHODOLOGY

A. Simulation details

We have carried out molecular dynamics simulations for systems of 1000 and 1728 molecules using the SPC/E potential function.[29] The equations of motion were solved with a fourth order gear predictor-corrector algorithm subject to cubic periodic boundary conditions. The time step was 1 fs. The Ewald sum[30] technique was used to handle long range electrostatic interactions. The study of density fluctuations and clustering requires the introduction of an effective density dependence. Since the SPC/E model is not density dependent, the isobaric conditions were introduced by varying the system volume (see Ref. 31). Following the work by Debenedetti and Errington we have performed simulations in the constant number of molecules, volume, and temperature (i.e., NVT) ensemble at temperatures 240, 260, 280, and 300 K and densities 0.984, 0.979, 0.974, and 0.9653 g/cm^3. These densities were calculated in the NPT simulations at atmospheric pressure by these authors[20] (1 atm) using the same potential function. This allows, albeit indirectly, the imposition of the required conditions on the canonical ensemble. Note that much larger systems (beyond our computational capabilities) are required in order to suppress the density fluctuations caused by a barostat in the NPT simulations.

Here we follow the original work of Debye[32] to compute the dielectric permittivity using the single dipole autocorrelation function $C(t)$

$$\epsilon(\omega)-n_\infty^2 \approx -\frac{4\pi N}{3kTV}\int_0^\infty \frac{d}{dt}C(t)e^{-i\omega t}dt \tag{3}$$

and the power absorption coefficient follows from the relation

$$\alpha(\omega)=\frac{2\omega}{c}\mathrm{Im}[\sqrt{\epsilon(\omega)}]. \tag{4}$$

In the relations (3) and (4), c is the velocity of light, μ is the dipole moment of the water molecule, N is the number of molecules in the volume V, T is temperature, and $C(t)=\langle \boldsymbol{\mu}(t)\boldsymbol{\mu}(0)\rangle$ is the single dipole auto correlation function (DACF); angle brackets indicate the ensemble average. The value of n_∞^2, the square of the index of refraction at infinitely high frequency, is not known for the SPC/E model and was chosen arbitrarily to be $n_\infty^2=1.0$.

Note that there exists a more rigorous expression for the calculations of dielectric permittivity of a molecular system with periodic boundary conditions.[33] It involves the total DACF, the use of which, however, does not allow a direct separation of the motion of water molecules inside the low density domains (in-cluster) and outside of them (off-cluster). The approach based on the expressions (3) and (4), albeit not as exact, can nevertheless reveal differences in the in-cluster and off-cluster contributions.

B. Cluster criterion

The scientific literature offers a few criteria for the identification of low density domains (hereafter we will refer to these as clusters) in ''computer water.'' We have examined several criteria to find the best one for our purpose. The first attempt was to use the integral of the distinct part of the van Hove function $G_d(r,t)$,

$$q_{r_c,\tau_v}=\int_0^{r_c}\int_0^{\tau_v} G_d(r,t)dt\,dr, \tag{5}$$

over a time interval τ_v and a range of intermolecular distances r_c. The value of r_c was chosen to be the position of the first minimum in the static oxygen-oxygen radial distribution function and the time τ_v was chosen to be 1 ps. We found that the procedure based on this approach is unstable. It appears that the integral (5) cannot be estimated accurately enough over the intervals specified. Our second attempt was to use a criterion based on the self part of the van Hove function.[21] The study in which this was introduced, focused on the most mobile molecules in the ensemble. We found that this definition is not appropriate for probing the apparently ordered domains, in which the translations are expected to be restrained. Finally we tried to employ the definition that has recently proved to be practical for Monte Carlo simulations of supercooled water.[20,34] This criterion is based on the order parameter q defined as

$$q(t)=1-\frac{3}{8}\sum_{j=1}^{3}\sum_{k=j+1}^{4}\left(\cos\psi_{jk}(t)+\frac{1}{3}\right)^2. \tag{6}$$

The calculations of this quantity involve the positions of a given (central) molecule and four nearest neighbors. The summation is carried out over all the angles ψ_{jk} (six possible combinations) formed by lines joining the oxygen atoms of any two peripheral molecules and the central molecule.[20] Note that the q value varies in the range between 0 and 1 and in a perfect tetrahedral environment $q=1$.

In the present work we use the integral of the order parameter as follows:

$$\overline{q}=\int_0^{\tau_v} q(t)dt/\tau_v. \tag{7}$$

Note that this definition is slightly different from what has been used previously. We extended it to be a time average (indicated by the bar) over a period that is much shorter than the characteristic time of the ''cage'' dynamics and much longer than the vibrational or librational period. The integration limit τ_v is chosen to be 0.5 ps, which is on the threshold between harmonic and cage dynamics (we discuss this further in the following section and Fig. 4). Thus $\overline{q}$ is the order

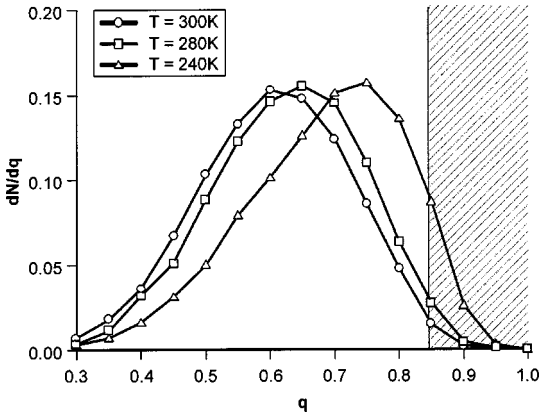

FIG. 1. The order parameter $\overline{q}$ probability distribution for H_2O molecules at different temperatures.

parameter for vibrationally averaged structures. This criterion has proven to be the best for the purposes of the present study.

The following conditions for clustering are used throughout this study: two molecules belong to the same cluster if they have a value of $\overline{q}$ greater than 0.85 and are separated by a distance less than 0.32 nm and those pairs of molecules that satisfy these two conditions are members of the same cluster if there is a path connecting them. The choice of the $\overline{q}$ value is to some extent subjective. The value of 0.85 is, however, a good choice in the sense that a substantial number of molecules possessing this value of $\overline{q}$ can be observed only at relatively low temperatures ($<$280 K) and approaches zero at 300 K. Since this property is not zero at room temperature, we consider the changes in this property relative to the room temperature value. The probability density for a molecule to posses a given $\overline{q}$ value is shown in Fig. 1 as a function of temperature. It can be seen that the fraction of molecules having $\overline{q} \geqslant 0.85$ is very small at 300 K.

IV. RESULTS AND DISCUSSION

In Fig. 2, we show the results of an analysis of the experimental extinction spectra. These are presented as volume size distribution functions for supercooled water droplets at 243 K (top plot) and ice crystals at 236 K (bottom plot). The top plot exhibits two modes. The majority of the liquid water volume is in small droplets with a mean radius of 1.5 μm, while a weaker mode of larger particles is centered at $\sim$4 μm. The nucleation rate constant at 243 K (see Ref. 14) is $\approx J = 4.3 \times 10^{-7}\ \mathrm{cm}^{-3}\ \mathrm{s}^{-1}$, which implies that 4 μm droplets would require about 10^{15} to 10^{16} s to freeze. The residence time—the average time that droplets spend in the cold sections before being probed by the FTS—is on the order of 10^3 s. Thus, we can safely state that the droplets are composed of liquid water.

The temperature at which the nucleation rate becomes large enough to freeze 4 μm particles rapidly is about 239 K, below which the liquid to crystal transition is very fast. The volume size distribution for the ice particles at 236 K shown in the bottom plot is centered at 4 μm. We detected a rapid growth of the population of large ice particles and simultaneous disappearance of the small mode of liquid water droplets at this temperature. This is caused by mass transfer—i.e., evaporation from the liquid and deposition onto the crystal—a phenomenon that is driven by the difference between the equilibrium vapor pressures over supercooled liquid water and ice. Water nucleation and freezing rate measurements will be the subject of future reports. We present these data here only to show that we can control the phases and, to some extent, sizes of water aerosols. Hereafter we will focus on supercooled liquid water particles at temperatures above 239 K.

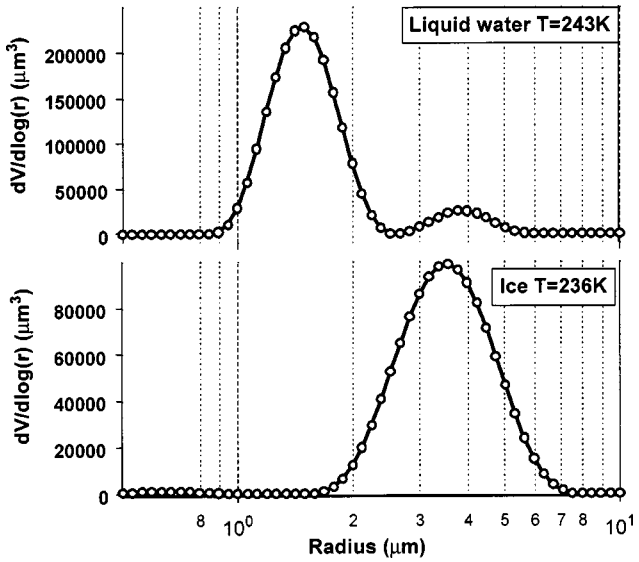

FIG. 2. Volume size distribution function for liquid water and ice retrieved from the extinction IR spectra.

The MD simulations have shown that the clusters that constitute the low density regions have rather open or chainlike linear structures (see Fig. 3). They become more compact with increasing size; thus five and six member rings are typical structural elements of the larger clusters ($>$40 molecules). More statistics (size distributions, number of hydrogen bonds per a cluster, etc.) for the SPC/E model can be found in Refs. 20 and 34. Here we focus on the molecular dynamics in these domains and their connection to the IR and microwave spectra. The extinction spectrum of supercooled water recorded at 243 K together with computed spectra obtained using our procedure are shown in Fig. 4. The figure illustrates the results of computations that use the

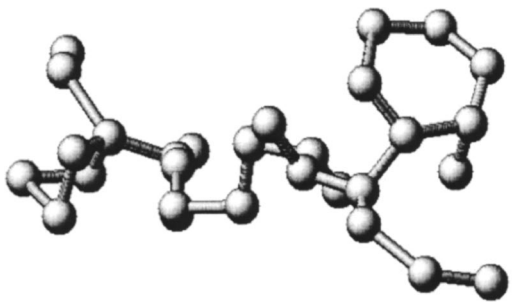

FIG. 3. The snapshot of the 30-members molecular assembly from MD simulation at 260 K with $q = 0.85$. Balls are the oxygen atoms. Poles are the bonds specified in accordance with the criterion used.

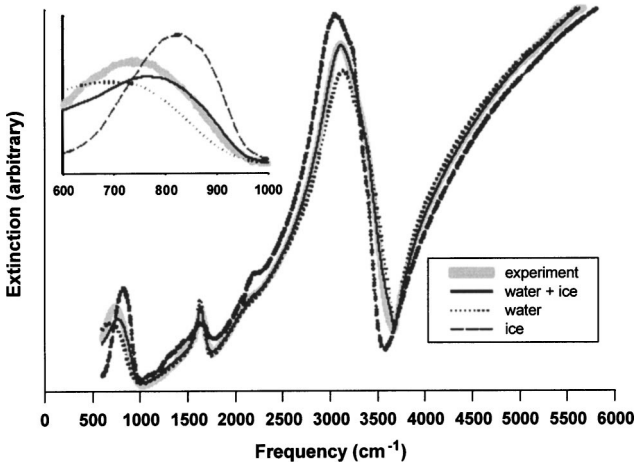

FIG. 4. Experimental extinction spectra together with their best fits.

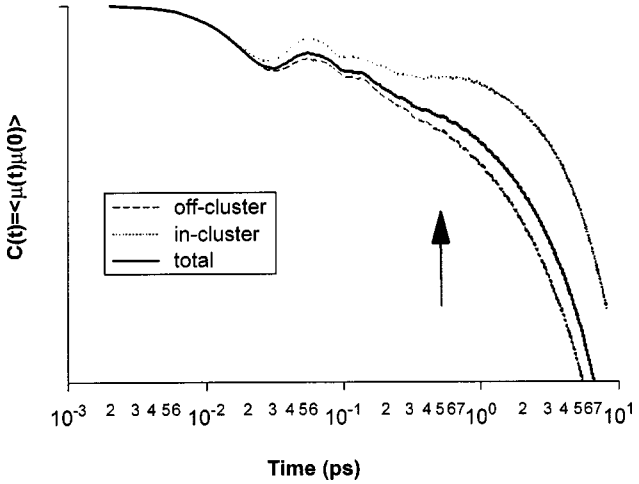

FIG. 5. Partial single dipole moment autocorrelation functions for H_2O molecules in- and off-the clusters. The total DACF is show as a reference. The arrow indicates the threshold between the harmonic and cage dynamics.

experimental refractive indices of (1) liquid water (measured at 298 K[19]); (2) ice (measured at 223–266 K[17]); and (3) the sum of the latter two. These results indicate clearly that the spectrum of supercooled water over a wide frequency range can be described most accurately by combining the refractive indices of ''warm'' water and relatively warm ice.

As we pointed out earlier, it is not possible for ice to have formed at the temperature of these observations. Moreover, supercooled water could not coexist with ice at this temperature for the residence time in the flow tube (about 1 min), because the entire sample would freeze in the presence of ice nuclei. The obvious improvement in the spectral fit achieved by the addition of ice refractive indices to the analysis suggests the presence of a component having absorption and scattering properties that are very similar to those of ice. We believe that this indicates, although indirectly, the existence of ordered (crystal-like) local environments in supercooled water.

The most pronounced temperature variations in the spectral densities occur in the low frequency range between 500 and 1000 cm^{-1} (see inset in Fig. 4). The figure shows the variations in the spectral density of librations (see, for instance, Ref. 35) of water molecules. The frequency and intensity of the librational mode depend strongly on the local molecular structure, and therefore are indicative of the presence of these low density domains, which is a central objective of the present work.

The spectral densities of librations were computed using Eqs. (3) and (4). The separation into the in-cluster and off-cluster contributions was achieved by initiating the single DACF computations on the molecules that initially belonged to the clusters. The off-cluster spectral contribution was computed similarly, by initiating and following the trajectories of the molecules that were initially off the low density domains. The partial (in-cluster, off-cluster, and total) DACFs are shown in Fig. 5. We found that the reorientations in domains are slower, which is manifested in a more gradual decay of the in-cluster DACF in comparison with that of the total. It is interesting to note that this resembles the temperature evolution of the Debye time τ_d. Here we can see at least two exponentials (in- and off-cluster) that result in generally non-Debye behavior of the total DACFs thus leading to a stretched exponent, so-called α process typically observed in supercooled liquids and glasses. Note that this occurs normally in glass forming liquids, in which the relaxation rates and diffusion vary through several orders of magnitude on cooling.

The power absorption spectra computed from these autocorrelation functions are shown in Fig. 6. The spectra exhibit two distinct regions: a translational mode centered at 100 cm^{-1} and a librational mode at around 600 cm^{-1}. The positions of the peaks agree well with instantaneous normal mode computations performed with the same potential model.[23] The spectra also agree reasonably well with the experimental spectra (see the top plot in Fig. 6), although all

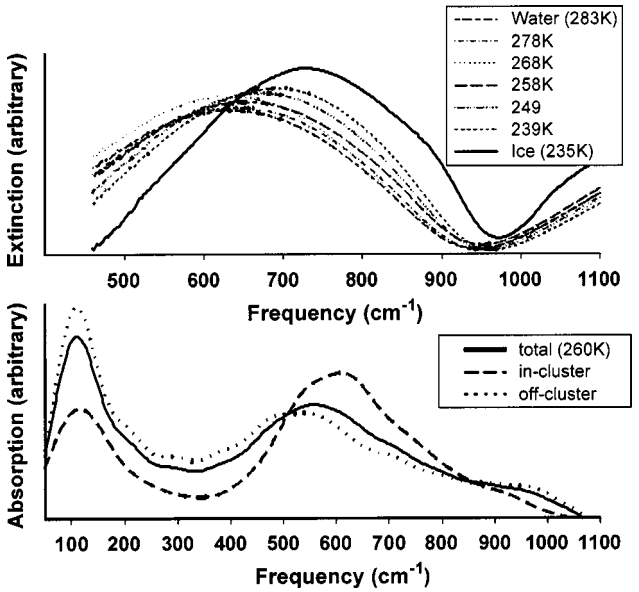

FIG. 6. Top panel presents the experimental extinction spectra of supercooled water over a range of temperatures. The bottom panel shows the power absorption spectra for water at 260 K computed using the MD simulations; in- and off-cluster contributions are shown by the dashed and dotted line, respectively.

the frequencies in the latter are shifted higher by about 80 cm^{-1}. These computed results provide insight into the dynamics in different local environments in cold water. The intensity of the translational mode shown in the lower panel of Fig. 6 is lower for the low density domains than for the average and off-cluster molecules, indicating some restriction on the translational motion of H_2O molecules. The peak of the librational mode, on the other hand, becomes higher and shifts toward higher frequencies with decreasing temperature, indicating the increasing spectral intensity of the librational motion as well as the increasing strength of the intermolecular interactions. Both of these are characteristic of increased ordering. As discussed above, the same pattern is evident in the experimental spectra of the librational mode, which are shown at the top of Fig. 6. We conclude that there is an increased ordering in the liquid as the temperature decreases. Combining this with the fact that the experimental spectra are more accurately reproduced by the combination of water and ice optical constants (see Fig. 4) suggests that these ordered regions have structures that are similar to ice. On the basis of this, we conclude that these low density domains are nascent crystal structures in which the molecules have reduced translational and increased rotational (librational) mobility as the temperature decreases.

The MD simulations reveal the fact that the low density (more structured) domains persist longer than the average cage. The temperature evolution of the reorientation time τ_1 can be elucidated by examining the slope (the dependence is linear on a logarithmic scale) of the single DACF. The microscopic dielectric relaxation time τ_d can be obtained from $\tau_d \approx 2\tau_1$.[36,37] Since the statistics from our MD simulations are not adequate to examine long time behavior of these reorientations and thereby verify that there is a nonexponential tail in the DACFs, we fitted the slope by a single exponential. The temperature dependence of the relaxation time, $\tau_1(T)$, can be approximated by a Gibbs-Adam type of relation.[38] These simulation results, however, do not exactly obey the Angell-Speedy relation[39] with a singularity temperature of 228 K. The right panel in Fig. 7 presents the calculated values of $2\tau_1$ in comparison with the experimental data for the Debye relaxation times τ_d. Clearly, the computed relaxation times are in good agreement with the recent experiments.[40,41]

The fraction f_L of the molecules that belong to the low density domains can be estimated roughly from the IR spectra using the evidence from the MD simulations. We use the sum of water and hexagonal ice to fit the experimental spectra, assuming that the refractive indices of the domains can be approximated by those of ice. At 300 K, the procedure gives a small ($f_L = 0.02$) fraction of structured domains, which rises to about 0.3 at 240 K. The values of f_L obtained from the IR experiment and the MD simulations are compared in Fig. 8. The results agree well in the sense that the curves have similar slopes and f_L reaches ≈ 0.3 at 240 K. As noted previously, we have subtracted the fraction at room temperature in each case to scale the results. The plausible reason for the offset in the case of the simulation results with the SPC/E model is that the stability region of 1 h ice is shifted by ≈ 13 to 260 K.[42]

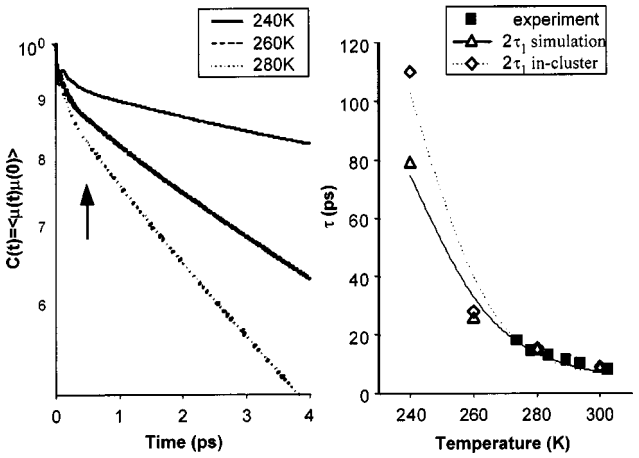

FIG. 7. Left panel shows the single dipole moment autocorrelation functions for supercooled water in a range of temperatures. The right panel shows the temperature dependence of the dielectric relaxation times (open triangles) obtained from the correlation functions shown in the left panel in comparison with the experimental data (Ref. 41) (solid squares). The reorientations in-clusters are slower than that of the total (open diamonds).

The suggestion that ordered domains exist in supercooled water droplets is also in agreement with the results of neutron scattering experiments.[24] The starts in Fig. 8 show results that we obtained by plotting $[\alpha(300\,\mathrm{K}) - \alpha(T)]$ values that we adapted from the 1 bar curve in Fig. 3 of Ref. 24, where $[1-\alpha]$ is the concentration of low density liquid. The relative increases in the structured fraction with decreasing temperature obtained using these three different techniques agree very well. Thus we can conclude that the fraction of the low density domains rises to about 0.3 over the temperature range from 300 to 240 K.

V. CONCLUDING REMARKS

In the present work we have considered the effect of density fluctuations on some dynamic and structural properties of liquid water in the framework of the concept of local heterogeneities that seemingly arise from the expansion and slow density fluctuations in water on cooling. We identified these domains based on a criterion proposed earlier[34] using

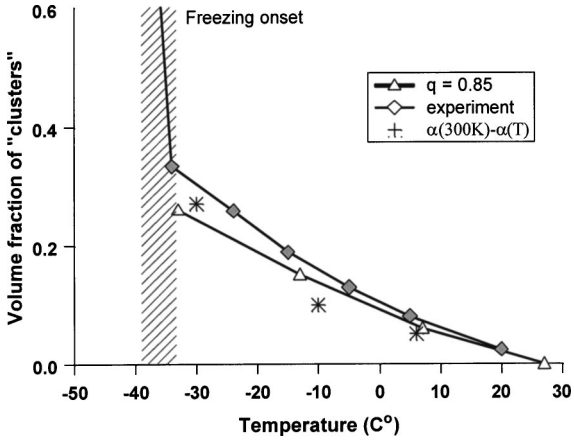

FIG. 8. Volume fraction of the low density domains in water as a function of temperature. Stars show the change of the ''low density liquid'' adapted from Ref. 24.

MD simulations. We also associate them with the ordered fraction, which we found by analyzing the infrared spectra of supercooled water droplets. The results obtained from the IR spectra and the MD simulations are consistent with the conclusion based on neutron scattering experiments.[24] All these approaches agree that the volume fraction of the ordered domains reaches a value of about 0.3 at 240 K (assuming that f_L equals zero at 300 K).

The dynamics in the low density domains in supercooled water was also examined. We found that with decreasing temperature, the librational mode at around 600 cm^{-1} grows, sharpens, and shifts toward higher frequencies. The shift of the peak position is $\approx$80 cm^{-1} in the temperature range between 240 and 300 K. The dielectric relaxation times obtained from MD simulations show that reorientations of low density molecules are somewhat slower than those of the bulk, indicating that the low density domains persist longer than the ''average'' local environment. The intensities of the translational mode for the molecules in the low density domains are reduced, whereas the frequencies of the librational mode are increased. In view of the fact that clustering processes are cooperative in nature, the above observations are indicative of the formation of ordered local structures closely resembling ice. Within this formalism, the spectral response of these domains can be assumed to be similar to that of ice.

We found that a relatively large fraction of molecules in supercooled water tend to assemble into multiple small (20 to 100 molecules) nuclei before freezing. If these are viewed as precritical nuclei, the freezing mechanism may then be interpreted as the extension of this process (formation of ordered domains) to a point where several domains have a nonzero chance to overlap thus forming a critical nucleus on which the crystalline ice lattice forms.

ACKNOWLEDGMENT

The authors are grateful for the financial support of the Natural Sciences and Engineering Research Council of Canada.

[1] Y. J. Kaufman, D. Tanre, and O. Boucher, Nature (London) **419**, 215 (2002).
[2] T. Peter, Annu. Rev. Phys. Chem. **48**, 785 (1997).
[3] S. Solomon, Rev. Geophys. **26**, 131 (1988).
[4] L. S. Bartell, J. Phys. Chem. B **101**, 7573 (1997).
[5] P. G. Debenedetti, J. Phys.: Condens. Matter **15**, R1669 (2003).
[6] F. Sciortino, E. La Nave, A. Scala, H. E. Stanley, and F. W. Starr, Eur. Phys. J. E **9**, 233 (2002).
[7] Y. S. Djikaev, A. Tabazadeh, and H. Reiss, J. Chem. Phys. **118**, 6572 (2003).
[8] L. B. Allen and J. L. Kassner, J. Colloid Interface Sci. **30**, 81 (1969).
[9] R. H. Heist and H. Reiss, J. Chem. Phys. **59**, 665 (1973).
[10] J. F. Huang and L. S. Bartell, J. Phys. Chem. **99**, 3924 (1995).
[11] V. B. Mikheev, P. M. Irving, N. S. Laulainen, S. E. Barlow, and V. V. Pervukhin, J. Chem. Phys. **116**, 10772 (2002).
[12] P. J. Demott and D. C. Rogers, J. Atmos. Sci. **47**, 1056 (1990).
[13] B. Kramer *et al.*, J. Phys. Chem. **111**, 6521 (1999).
[14] H. R. Pruppacher and J. D. Klett, *Microphysics of Clouds and Precipitation* (Kluwer Academic, London, 1998).
[15] P. Stockel, H. Vortisch, T. Leisner, and H. Baumgartel, J. Mol. Liq. **96-7**, 153 (2002).
[16] O. Jourdan, S. Oshchepkov, J. F. Gayet, V. Shcherbakov, and H. Isaka, J. Geophys. Res., [Atmos.] **108**, 4572 (2003).
[17] S. G. Warren, Appl. Opt. **23**, 1206 (1984).
[18] M. L. Clapp, R. E. Miller, and D. R. Worsnop, J. Phys. Chem. **99**, 6317 (1995).
[19] J. E. Bertie and Z. D. Lan, Appl. Spectrosc. **50**, 1047 (1996).
[20] J. R. Errington, P. G. Debenedetti, and S. Torquato, Phys. Rev. Lett. **89**, 215503 (2002).
[21] N. Giovambattista, S. V. Buldyrev, F. W. Starr, and H. E. Stanley, Phys. Rev. Lett. **90**, 085506 (2003).
[22] G. G. Malenkov, D. L. Tytik, and E. A. Zheligovskaya, J. Mol. Liq. **106**, 179 (2003).
[23] F. Sciortino and P. Tartaglia, Phys. Rev. Lett. **78**, 2385 (1997).
[24] M. C. Bellissent-Funel, Nuovo Cimento D **20**, 2107 (1998).
[25] A. K. Bertram, D. B. Dickens, and J. J. Sloan, J. Geophys. Res., [Atmos.] **105**, 9283 (2000).
[26] G. Bohren and D. Huffman, *Absorption and Scattering of Light by Small Particles* (Wiley, New York, 1983).
[27] B. L. Phillips, J. Assoc. Comput. Mach. **9**, 84 (1962).
[28] C. L. Lawson and R. J. Hanson, *Solving Least Squares Problem* (Prentice-Hall, Englewood Cliffs, 1974).
[29] H. J. C. Berendsen, J. R. Grigera, and T. P. Straatsma, J. Phys. Chem. **91**, 6269 (1987).
[30] M. P. Allen and D. J. Tildesley, *Computer Simulation of Liquids* (Oxford, New York, 1989).
[31] F. H. Stillinger, H. Sakai, and S. Torquato, J. Chem. Phys. **117**, 288 (2002).
[32] P. Debye, *Polar Molecules* (Chemical Catlog, New York, 1929).
[33] J. M. Caillol, D. Levesque, and J. J. Weis, J. Chem. Phys. **85**, 6645 (1986).
[34] J. R. Errington and P. G. Debenedetti, Nature (London) **409**, 318 (2001).
[35] J. P. Devlin, J. Sadlej, and V. Buch, J. Phys. Chem. A **105**, 974 (2001).
[36] T. W. Nee and R. Zwanzig, J. Chem. Phys. **52**, 6353 (1970).
[37] A. Rahman and F. H. Stillinger, J. Chem. Phys. **55**, 3336 (1971).
[38] G. Adam and J. H. Gibbs, J. Chem. Phys. **43**, 139 (1965).
[39] R. J. Speedy and C. A. Angell, J. Chem. Phys. **65**, 851 (1976).
[40] C. Ronne, L. Thrane, P. O. Astrand, A. Wallqvist, K. V. Mikkelsen, and S. R. Keiding, J. Chem. Phys. **107**, 5319 (1997).
[41] C. Ronne and S. R. Keiding, J. Mol. Liq. **101**, 199 (2002).
[42] S. C. Gay, E. J. Smith, and A. D. J. Haymet, J. Chem. Phys. **116**, 8876 (2002).